Reflected Shock Experiments on the Equation-of-State Properties of Liquid Deuterium at 100–600 GPa (1–6 Mbar)

A. N. Mostovych,[1] Y. Chan,[2] T. Lehecha,[2] A. Schmitt,[1] and J. D. Sethian[1]
[1]*Laser Plasma Branch, Plasma Physics Division, U.S. Naval Research Laboratory, Washington, D.C. 20375*
[2]*Science Applications International Corporation, McLean, Virginia 22102*
(Received 7 January 2000)

New laser-driven shock experiments have been used to study the equation-of-state (EOS) properties of liquid deuterium. Reflected shocks are utilized to increase the shock pressure and to enhance the sensitivity to differences in compressibility. The results of these experiments differ substantially from the predictions of the Sesame EOS. EOS models showing large dissociation effects with much greater compressibility (up to a factor of 2) agree with the data. By use of independent techniques, this experiment offers the first confirmation of an earlier observation of enhanced compressibility in liquid deuterium.

PACS numbers: 64.30.+t, 62.50.+p

The properties of hydrogen and its isotopes at high pressure and high density are important to current issues in planetary structure, inertial confinement fusion (ICF), and to the physics of condensed matter. At pressures in the range of 50 GPa and above hydrogen is expected to change from a molecular to a metallic or strongly coupled plasma state [1]. This transition region is not well understood and current theoretical models for the equation of state (EOS) of hydrogen vary substantially in their predictions [2–5]. These discrepancies are particularly important for shock compression because they lead to a 40% uncertainty in the compressibility of hydrogen. This level of uncertainty is significant for the design of ICF shock driven deuterium-tritium pellets [6] and for the planetary models of Jupiter [7]. Controlled experiments under these conditions are difficult to field, and there exists only one set of data from recent shock experiments on the Nova Laser Facility [8]. These experiments used x-ray radiography and laser interferometry to measure the Hugoniot (EOS) of deuterium. They found large increases in deuterium compressibility at pressures between 50 and 200 GPa, but current theory cannot reproduce these results from first principle calculations.

In this Letter, we report on new deuterium shock wave experiments in which the EOS of deuterium is probed with laser-driven shocks, reflected from an aluminum reference anvil. Reflected shock techniques [9] are used to increase the available pressure and to help evaluate the EOS properties of deuterium in terms of aluminum. Aluminum is a well understood material for which a significant body of data is available. This approach does not require any assumptions about the optical or x-ray refractive properties of the shock front and does not suffer from parallax errors of side-view diagnostics. For 50–200 GPa pressures in the primary shock and 100–600 GPa in the reflected shock we found that the data do not agree with standard Sesame EOS tables [3] but are best described by equations of state which have large increases in compressibility in the 50 to 200 GPa region. The results are in agreement with the predictions of the linear-mixture model of Ross [4] and the experimental results of Da Silva *et al.* [8].

The Nike KrF laser is used to drive the high pressure shocks in this work [10]. This laser uses induced spatial incoherence [11] to generate very smooth, flat-topped, illumination profiles on target ($\delta I/I < 0.02$). This is needed to drive steady, well-controlled, and planar shocks. As per Fig. 1, multiple beams of the Nike laser are focused to a 750–1250 μm spot on target. With 40 overlapped beams and up to 50 joules per beam the targets are driven with an intensity of 10^{13}–10^{14} W/cm^2 over a duration of 4–5 ns.

The target capsule, shown in Fig. 1, consists of an aluminum pusher, a deuterium payload region, and an aluminum witness plate anvil. The target capsule is mounted in a miniature copper cryostat filled with liquid deuterium at a temperature of 20 K [12]. The aluminum pusher is driven with laser beams through a thin (10–13 μm) layer of Kapton. Laser ablation of the Kapton layer generates high pressures, driving a 500 to 800 GPa shock into the

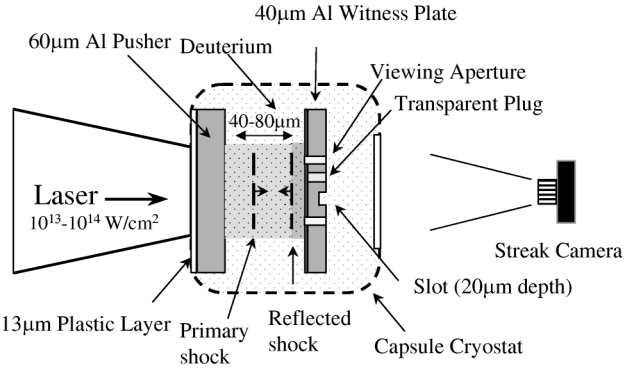

FIG. 1. Schematic of a reflected shock experiment in liquid deuterium. A high intensity laser drives an aluminum pusher plate to launch a strong shock wave inside a deuterium filled target capsule. The shock propagates across the deuterium gap and is reflected from an aluminum witness plate. A high speed streak camera is used to measure the speed of the shock and the strength of the reflected shock.

 0031-9007/00/85(18)/3870(4)$15.00

aluminum pusher. The laser radiation is fully adsorbed in this layer, effectively shielding the aluminum pusher. We do not illuminate the aluminum directly because aluminum is known to produce high levels of penetrating x rays that preheat and perturb the target capsule. The dominant x rays from the atoms in Kapton (C, H, N, O) have energies below 2.6 keV. They are promptly stopped in the leading edge ($1/e \sim 3.5$ μm) of the aluminum pusher. Steady shock propagation is ensured by making the pusher thick enough to prevent preheat and to permit dissipation of initial pressure transients before they reach the aluminum-deuterium interface. We conducted experiments with special multistep targets to prove that 60 μm of Al in a pusher plate is sufficient to launch and maintain steady drive pressure for the duration of the shock travel in the deuterium and the witness plate [13]. As a result, it is assumed that the shock is steady during this time. As the shock exits from the aluminum pusher and releases into the liquid deuterium, the deuterium is compressed and shocked to pressures of 50–300 GPa. The deuterium shock propagates across the gap (40 or 80 μm) in the target capsule and impacts a thin ($\sim$40 μm) aluminum witness plate. After impact, the deuterium shock reflects from the higher impedance aluminum plate and transmits a shock into it. Because of the continuity of pressure across the interface, the reflected and transmitted shocks are at the same pressure (200–600 GPa).

The interactions of the shocks in the target capsule are best analyzed by examining the Hugoniot EOS curves for deuterium and aluminum. The Hugoniot EOS is a subset of the EOS phase space [14], which can be accessed by a shock wave under the conditions of conservation of energy, momentum, and mass. Figure 2 displays the appropriate primary and reflected Hugoniot curves as a function of flow velocity and pressure behind the shocks. The two lower curves, originating from atmospheric pressure, are the primary Hugoniot curves for deuterium, calculated from the NRL Gardner-Hazak (G-H) EOS model [5], with and without dissociation. At the point of reflection from the aluminum witness plate the two models predict different flow velocities for an initial shock ($V_s = 2.65 \times 10^6$ cm/sec in this example) and very different reflected Hugoniot curves. The pressure and the flow velocity must be conserved across the aluminum-deuterium interfaces; thus the intersection of the reflected curves with the primary aluminum Hugoniot curve determines the pressure in the reflected shock. The pressure difference in the reflected shock is large and corresponds to a large difference in compressibility as shown in Fig. 3. This allows for a simple but sensitive test for differences in the EOS.

The experiment measures the pressure of the reflected shock as a function of the initial shock velocity in the deuterium. The witness plate functions as an anvil to reflect the shock and an indicator to mark the time it takes the shock to cross the gap. The aluminum witness plate has three diagnostic holes that are used to probe the shock in the target interior. Two open holes give a clear view of the rear side of

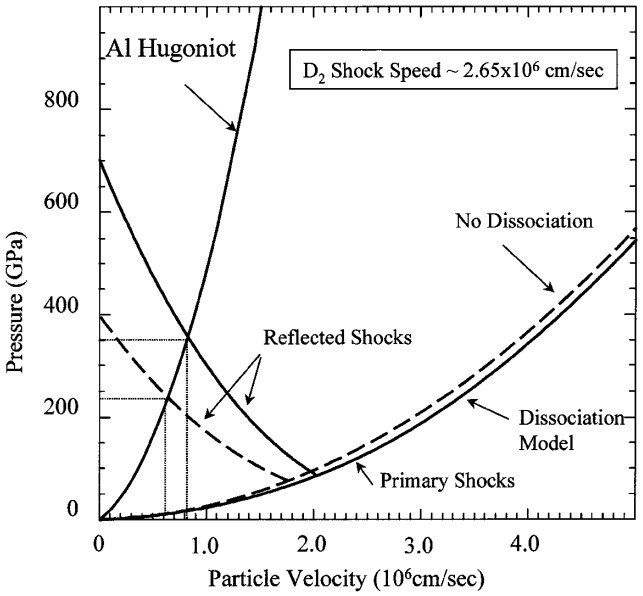

FIG. 2. Hugoniot curves and matching conditions for deuterium and aluminum shocks. The shock reflection properties are sensitive to the treatment of dissociation in the equation of state models. The deuterium curves are due to the NRL (G-H) EOS model [5] with and without dissociation. As a result of the conservation of pressure and mass flow across the Al-deuterium interface, the pressure in the reflected shock is determined by the points where the reflected curves cross the aluminum curve.

the aluminum pusher. At the time of shock breakout from the aluminum pusher the surface heats to about 10 000 K and emits strongly in the visible and ultraviolet. The shock breakout signals are recorded with a fast streak camera observing the target from the rear. The third hole is filled with a clear polymer having a thin ($\sim$1000 Å) but opaque aluminum indicating layer on top of the polymer. The indicating layer is on the inside surface of the witness plate. As the deuterium shock impacts the witness plate, it also impacts the indicating layer at the same time. The indicator heats up and radiates, indicating the time of shock arrival. The shock speed is determined from the known dimensions of the gap and the measured transit time across the gap. The pressure of the reflected and transmitted shocks is determined from the speed of the transmitted shock in the witness plate [$v_s \sim (1-2) \times 10^6$ cm/sec] and the known EOS properties of aluminum. The exiting shock from the witness plate is recorded in a thin region ($\sim$20 μm) of the plate, in a slot at the rear. The witness plate must be thin in order to prevent higher order shocks, originating from multiple reflections between the aluminum pusher and the witness plate, from catching the first shock through the plate. Higher order shocks are visible in the streak camera images as an additional breakout after the first transmitted shock breaks out of the witness plate. The slot allows the effective thickness to be small while maintaining structural integrity. A typical streak camera image of all the shock breakouts is displayed in Fig. 4.

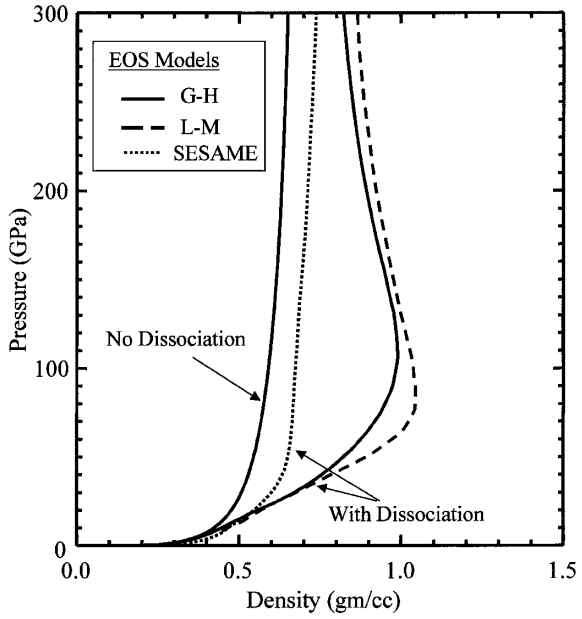

FIG. 3. The primary Hugoniot curves for deuterium as a function of density and pressure. Dissociation introduces additional degrees of freedom that result in increased compressibility. The (G-H) Gardner-Hazak model treats dissociation as a simple mass-action reaction between monotomic and diatomic states. The (L-M) linear mixing model treats dissociation as a transition between diatomic and semimetallic states. Both models contain free parameters which are constrained by previous experiments.

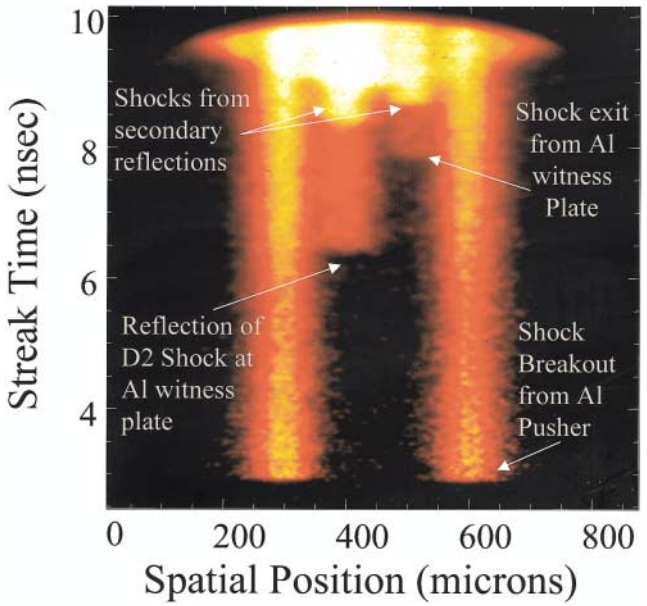

FIG. 4 (color). Streak camera record of a typical emission signal from the reflected shock experiment. As per Fig. 1, the emission is detected from diagnostic holes in the target capsule. The emission starts as the shock in the aluminum pusher breaks out into the deuterium. The simultaneity and flatness of this emission signal reflects the flatness of the pressure profile driven by the laser. The second and third steps correspond to the times when the shock collides with the witness plate and when the transmitted shock exits the aluminum witness plate. [$I_{\text{laser}} \sim 5 \times 10^{13}$ W/cm^2, $V_s(\text{D}_2) \sim 2.3 \times 10^6$ cm/sec, $V_s(\text{Al}) \sim 1.65 \times 10^6$ cm/sec.]

The target pusher and witness plates are micromachined from solid aluminum and assembled in the target capsule. The positions of the witness plate and pusher surfaces and the depth of the slot are determined by white light interferometry to an accuracy of 0.1 μm. The witness plate thickness is determined, before assembly, by measurements of the area and mass of the plates. Changes in the target dimensions at liquid deuterium temperatures are calculated using the known expansion curves of aluminum between 20–300 K. These changes are very small and unimportant. The witness plate is completely immersed in the pool of liquid deuterium to ensure that all surface tension forces are balanced. Extensive tests were conducted to ensure that the glue joints in the target were not broken by the thermal cycle from 300 to 20 K. Deuterium initial state conditions are obtained from measurements of the cryostat temperature and plenum pressure before each shot. The initial density is determined from these measurements and the known low-pressure EOS of cryogenic deuterium [15]. For accurate time measurements, the streak camera is calibrated with a train of short duration laser pulses, derived from multiple reflections between two mirrors.

Measurements of the reflected shock pressure are plotted as a function of initial shock velocity in Fig. 5. The shock strength was controlled by changes in the laser intensity through a variation of the laser energy and spot size. The fundamental errors in the experiment are due to uncertainties in the dimensions of the deuterium gap, the thickness of the witness plate, and the timing accuracy of the shock breakout signals. The uncertainty in the deuterium shock velocity is about 5% ($\Delta x/x \sim 1.25\%$, $\Delta t/t \sim 5\%$), whereas the velocity in the aluminum witness plate is more uncertain with $\Delta v/v \sim 15\%$ where $\Delta x/x \sim 7.5\%$ and $\Delta t/t \sim 13\%$. These errors are random and correspond to the best estimates of the standard deviation. In the regions of many data points a Gaussian distribution with $\sigma \sim 15\%$ accurately characterizes the spread in the data. The main systematic errors, the streak camera sweep speed accuracy ($\sim$0.5%) and the accuracy of the white light interferometer ($\sim$1%), are small in comparison. Shock planarity in the region between the two outermost observation holes was required for all data. Shots with nonuniform breakout or poor centering were rejected. The curves along the data are generated from reflected Hugoniot calculations, as per the example in Fig. 2. Separate matching conditions are solved for each value of the initial shock speed and the curves are the locus of points corresponding to those solutions. This is done for the Sesame equation of state [3], for the linear-mixing (L-M) model of Ross [4], and for the (G-H) EOS model with and without dissociation [5]. The (G-H) model treats dissociation as a simple mass-action reaction between monotomic and diatomic states, whereas the (L-M) model treats dissociation

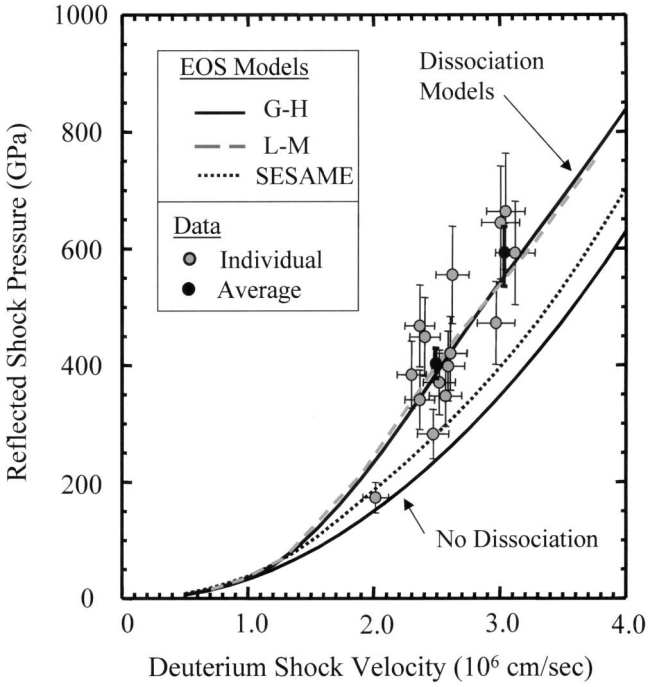

FIG. 5. Measurements of reflected shock pressure as a function of the primary shock velocity. The data are compared to the Sesame EOS tables and to EOS models that have increased compressibility as a result of dissociation. The data agree with the (L-M) [4] and (G-H) [5] dissociation models, indicating that liquid deuterium is much more compressible than predicted by the Sesame EOS tables. The two main groupings of points are averaged and shown as the filled points.

as a transition between diatomic and semimetallic states. Both models contain free parameters which are constrained by previous experiments [gas gun shock data [16] for the (L-M) model and Nova EOS experiments [8] for the (G-H) EOS model]. Dissociation introduces additional degrees of freedom that act as energy sinks and increase the compressibility. The Sesame equation of state also includes dissociation; however, it is not very sensitive to it. In contrast, the (L-M) and (G-H) models predict higher reflected shock pressures and substantially higher compressibility in deuterium. The data show that the standard Sesame EOS is not well suited in this pressure range. Instead, the data are in agreement with the high compressibility dissociation models for the equation of state.

In summary, we have fielded new experiments using techniques independent of those in the Nova experiments to test EOS models of liquid deuterium under conditions of high pressure. These measurements were done in the pressure range (50 to 600 GPa) that is important to the design of ICF experiments and the understanding of the planetary structure of large planets such as Jupiter. Our results are in agreement with EOS models that predict strong enhancement to the compressibility as a result of dissociation processes in this pressure range.

The authors acknowledge and thank M. Ross for the (L-M) model Hugoniot calculations, J. Dahlburg for hydrodynamic simulations, S. Bodner, J. Gardner, S. Obenschain, and A. Velikovich for extensive and fruitful discussions, the Nike laser and target teams for Nike operations, and Tom Walsh and his team at the Schafer Corporation for target manufacturing. This work is supported by the Department of Energy.

[1] H. Kitamura and S. Ichimaru, J. Phys. Soc. Jpn. **67**, 950 (1998); N. W. Ashcroft, Phys. World **8**, 43 (1995); S. Ichimaru, *Statistical Plasma Physics: Condensed Plasmas* (Addison-Wesley, New York, 1991).

[2] D. Saumon, G. Chabrier, and H. M. Van Horn, Astrophys. J. Suppl. Ser. **99**, 713 (1995); W. R. Magro, D. M. Ceperley, C. Pierleoni, and B. Bernu, Phys. Rev. Lett. **76**, 1240 (1996); T. J. Lenosky, J. D. Kress, and L. A. Collins, Phys. Rev. B **56**, 5164 (1997); F. J. Rogers, Astrophys. J. **310**, 723 (1986); R. M. More, K. H. Warren, D. A. Young, and G. B. Zimmerman, Phys. Fluids **31**, 3059 (1988); J. Lenosky *et al.,* Phys. Rev. B **61**, 1 (2000); G. Galli *et al.,* Phys. Rev. B **61**, 909 (2000).

[3] G. I. Kerley, in *A Theoretical Equation of State for Deuterium,* National Technical Information Service, Springfield, VA, 1972), NTIS Document No. LA-47766.

[4] M. Ross, Phys. Rev. B **58**, 669 (1998).

[5] J. H. Gardner and G. Hazak, Naval Research Laboratory Report No. NRL/MR6440-97-7967, 1997.

[6] J. D. Lindl, Phys. Plasmas **2**, 3933 (1995).

[7] D. J. Stevenson, J. Phys. Condens. Matter **10**, 11 227 (1998); W. J. Nellis, Chem. Eur. J. **3**, 1921 (1997); W. B. Hubbard, Science **214**, 145 (1981); R. Smoluchowski, Nature (London) **215**, 691 (1967).

[8] G. W. Collins *et al.,* Phys. Plasmas **5**, 1864 (1998); R. Cauble *et al.,* Phys. Plasmas **4**, 1857 (1997); L. B. Da Silva *et al.,* Phys. Rev. Lett. **78**, 483 (1997).

[9] W. J. Nellis, F. H. Ree, M. van Theil, and A. C. Mitchell, J. Chem. Phys. **75**, 3055 (1981).

[10] S. P. Obenschain *et al.,* Phys. Plasmas **3**, 2098 (1996).

[11] R. H. Lehmberg and S. Obenschain, Opt. Commun. **46**, 27 (1983).

[12] J. D. Sethian *et al.,* Phys. Plasmas **6**, 2089 (1999).

[13] A. N. Mostovych *et al.,* Naval Research Laboratory Report No. NRL/MR6731-99-8420, 1999.

[14] Ya. B. Zeldovich and Yu. P. Raizer, *Physics of Shock Waves and High-Temperature Hydrodynamic Phenomena* (Academic Press, New York, 1964).

[15] P. C. Souers, *Hydrogen Properties for Fusion Energy* (University of California Press, Berkeley, 1986).

[16] N. C. Holmes, M. Ross, and W. J. Nellis, Phys. Rev. B **52**, 15 835 (1995).